

Molecular dynamics simulation of polyethylene on single wall carbon nanotube

Hua Yang, Yong Chen, Yu Liu,^{a)} and Wen Sheng Cai

Department of Chemistry, State Key Laboratory of Elemento-Organic Chemistry, Nankai University, Tianjin 300071, People's Republic of China

Ze Sheng Li

State Key Laboratory of Theoretical and Computational Chemistry, Institute of Theoretical Chemistry, Jilin University, Changchun 130061, People's Republic of China

(Received 21 March 2007; accepted 9 July 2007; published online 4 September 2007)

Molecular dynamics simulations are carried out on the isothermal crystallization process of single polyethylene chains with different chain lengths on the single wall carbon nanotube. This process is summarized as two steps, i.e., adsorption and orientation, and the bond-orientational order parameter is used to show the details of this process. The results show that the attractive van der Waals interactions control the adsorption and orientation of polyethylene on single wall carbon nanotube, and as the chain length increases, more microstructures appear in the last ordered structure. The stems of the ordered structure align parallel to the single wall carbon nanotube axis. © 2007 American Institute of Physics. [DOI: 10.1063/1.2768060]

I. INTRODUCTION

Carbon nanotubes (CNTs) have recently attracted much attention due to their extraordinary electrical and mechanical properties,^{1–6} which potentially enabled CNTs to be widely applied in the fields of electronic and nanodevices. Generally, these applications require the noncovalent functionalizations of CNTs by organic molecules^{7,8} or polymers.⁹ For example, Li *et al.*^{10,11} used the crystalline polymers to functionalize CNTs via the CNT-induced polymer crystallization and they found a periodical pattern of polymeric materials on CNTs. The polymer crystallization has been an important topic over the past several decades.^{12–15} However, the mechanism of polymer crystallization is still under debate.^{14,16} The classical picture is that the crystalline lamellae are formed by primary nucleation and growth of stems on the crystal front. Recently, Strobl^{17,18} discussed the crystallization in the melt and suggested another picture, that is, the polymer crystallization should be a stepwise process. Because it is difficult to observe the molecular structural changes of polymers on CNTs directly through experimental methods, we try to use the computer simulation to investigate polymer crystallization process on CNTs.

Computer simulation has been widely regarded as a powerful tool for investigating the microscopic dynamics behavior of polymer crystallization. The crystallization of *n* alkanes has been studied by molecular dynamics^{19–34} (MD) or Monte Carlo (MC) simulations.^{35–37} Kavassalis and Sundarajan¹⁹ showed the folding of a single, isolated polyethylene chain via a “global collapse” mechanism. Fujiwara and Sato²⁰ studied the isolated chain and showed that an orientationally ordered globular structure consisting of a single polyethylene chain could be formed from a random

coil by gradual stepwise cooling. Zhang *et al.*²¹ and Fujiwara and Sato²² reported the reorganization of lamellar structure of a single polyethylene (PE) chain during heating. Zhang *et al.*^{23–25} reported that the precisely controlled branches in branched PE are argued to play an important role during the crystallization process of branched PE. Moreover, the behavior of a single long chain PE on a solid surface was discussed by Guo *et al.*²⁶ Meyer and Müller-Plathe^{27,28} performed simulations using a mesoscopic bead-spring model and showed that chain stiffness alone, without an attractive potential, is sufficient to induce the formation of chain-folded lamellae even in the melt. Recently, Muthukumar and co-workers^{30–32} studied many flexible polymer molecules undergoing crystallization from solutions. These simulations reveal molecular mechanisms of nucleation and growth, and the accompanying free energy barriers, during the very early stages of crystallization. Yamamoto³⁴ has reported in a series of papers on the crystal growth of polymers with special focus on polymer behavior at the crystal surface, either at crystal-vapor or crystal-melt interfaces by MD. However, to the best of our knowledge, the behavior of PE on CNTs has not been reported theoretically up to now.

Many works^{19–26} focused on single polymer chain to study the polymer crystallization process. In this paper, we carried out molecular dynamics simulation on the physical interactions between a PE chain and a single wall carbon nanotube (SWCNT). All of the investigations are concerned with the effect of polymer-surface and polymer-polymer interactions. Thus, like in Refs. 26 and 38 we neglect the solvent effect. It is our special interest to show the structural changes of PE on SWCNT surface, the effect of van der Waals (vdW) interactions on the structure of PE on SWCNT, as well as the relation between PE chain length and the last ordered structure, which will favor our understanding of this important, but less investigated, area of theoretical chemistry.

^{a)} Author to whom correspondence should be addressed. FAX: +86-22-2350-3625. Electronic mail: yuliu@nankai.edu.cn

II. MODELS AND SIMULATION METHODS

We use MD simulations to study four different chain lengths of a united atom PE model in contact with a single wall carbon nanotube. We first build three-dimensional-periodical SWCNT(10,10) and a nonperiodical amorphous PE chain by varying the rotational torsion using a random method, respectively. Then, we put the PE chain and the SWCNT(10,10) on the same model and try to move the amorphous PE chain to get a maximum contact with the SWCNT(10,10). Therein, four selected PE chain models, which have a different number of CH₂ units (only two CH₃ units lie on the head and the tail of each PE chain, respectively), were denoted as PE300-10-10 (600CH_x), PE500-10-10 (1000CH_x), PE750-10-10 (1500CH_x), and PE1000-10-10 (2000CH_x). The parameters of the periodical box were $a=b=160.91$ Å and $c=122.98$ Å. This made the PE chain on an infinite long SWCNT. Both a and b are long enough to ensure that PE is not being affected by its images in these two directions, and c equals to the length of SWCNT. Therefore, the behavior of PE chain may only be affected by its images in the c direction.

Like in Refs. 19–26, we treated CH_x group as a united atom to simplify the calculations. The Dreiding force field³⁹ has been successfully used in the investigations on the mechanism of polymer crystallization.^{19–26} Thus, we choose Dreiding force field in our simulations. The CH_x groups use the potential of Dreiding force field; the SWCNT(10,10)-carbon atoms adopt the same potential as the aromatic carbon atom in the Dreiding force field. The parameters used in the Dreiding force field are listed in Ref. 39. The total potential energy (E_{total}), which includes the bonding energy (E_{bond}) and nonbonding energy (E_{nonbond}), can be expressed as

$$E_{\text{total}} = E_{\text{bond}} + E_{\text{nonbond}} = E_b + E_\theta + E_\phi + E_{\text{vdW}}, \quad (1)$$

where E_b is the bond stretching energy, E_θ is the valence angle bending energy, E_ϕ is the dihedral torsion energy, and E_{vdW} is the van der Waals interaction energy.

Before the MD simulations, 500 steps of energy minimization were performed to remove local unfavorable structures. During this minimization, the positions of the carbon atoms in the SWCNT are fixed. The degrees of freedom belonging to the PE chain are allowed to move. Subsequently, MD simulations of 2000 ps were performed by using the *NVT* ensemble with a time step of 1 fs at 300 K. A cutoff distance of 12 Å with a buffer length of 0.5 Å was adopted to reduce the calculation of van der Waals interactions. Nose-Hoover's method was employed to keep the temperature of the system constant.^{40–42} To ensure the reliability of the results, we simulated systems with different initial configurations (we got similar result from different initial configurations) and repeated every simulation once. All the simulations were performed using CERIUSt² and MATERIAL STUDIO software packages from Accelrys, Inc.

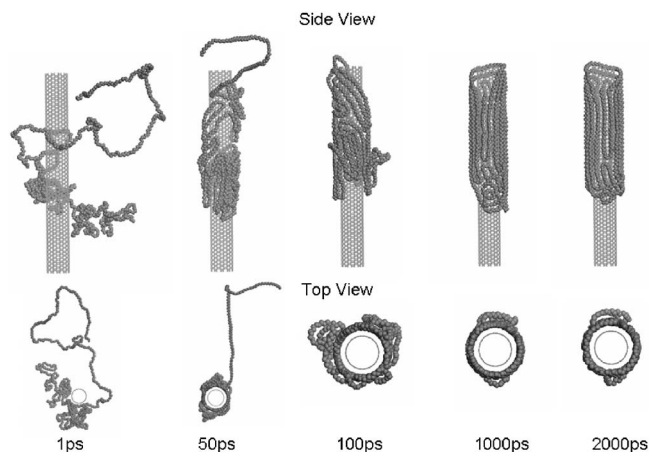


FIG. 1. Relaxation process of PE500 chain starting from random coil on SWCNT(10,10) surface at 300 K.

III. RESULTS AND DISCUSSION

A. Process of isothermal crystallization of PE chain

Many previous simulations focused on PE or PE-like polymer crystallization in bulk or on flat surface.^{19–33} To gain further understanding of the crystallization behavior of PE molecule, we discuss the relaxation process of a PE chain on a carbon nanotube surface. Figure 1 shows a typical relaxation process of PE500 chain starting from a random coil on SWCNT(10,10) surface at 300 K. It can be seen that the relaxation process of PE500 has some similarities with the PE chain relaxation on graphite surface.²⁶ Firstly, segments near the SWCNT anchor onto the SWCNT surface. Subsequently, the adsorbed segments are displaced along the SWCNT surface, and drag their neighboring segments onto the SWCNT surface. With more and more segments being dragged onto the SWCNT surface, the PE chain forms a layerlike structure until almost all the segments contact

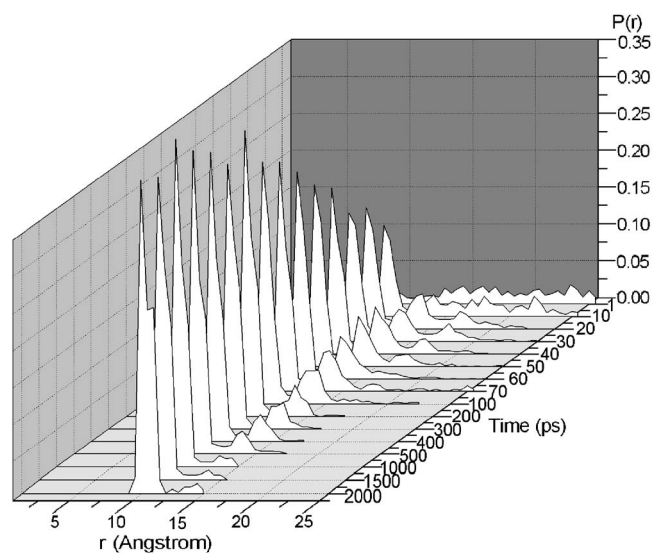


FIG. 2. Time evolution of radial density distribution function $P(r)$ for PE500-10-10 (its time axis is not linear).

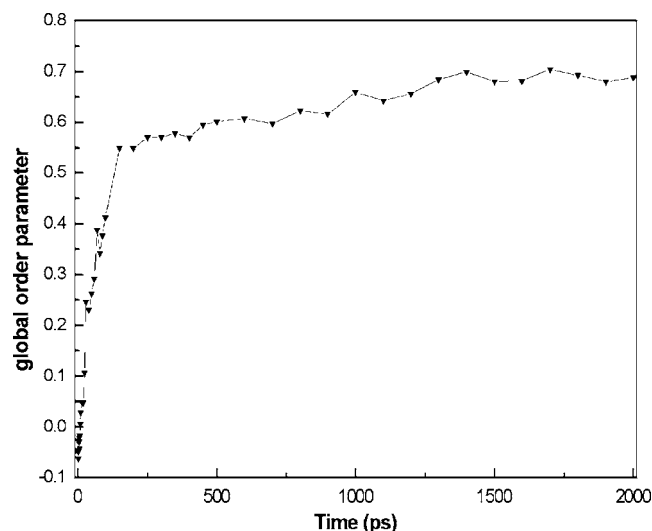


FIG. 3. Global bond-orientational order parameter A of PE on SWCNT(10,10) vs simulation time t .

SWCNT. Finally, the layerlike structure changes into ordered lamellae. The simulations of PE (Ref. 43) or *b*-PE (Ref. 23) show that subglobule will appear during the polymer chain relaxation, which is considered as crystal nucleation. We can

see “baby nuclei” similar to the work of Muthukumar.³² However, as the adsorption to the SWCNT is very strong, these small nuclei do not dominate the initial stage. Therefore, the process can be summarized as two steps, i.e., adsorption step and orientation step. The PE chains in the ordered lamellae are found parallel to the SWCNT axis, which is well consistent with the experimental result.⁷ For longer chains, more of such nuclei are expected to be found, which is validated by our simulation results for PE1500.⁴⁴

Radial density distribution function $P(r)$ is defined as the probability of finding CH_x at a distance r from the middle tube axis. In order to describe well the adsorption process of PE on SWCNT, we calculate $P(r)$ for PE500-10-10 and represent the time evolution of $P(r)$ in Fig. 2. CH_x has a wide distribution when the relaxation begins. As the simulation proceeds, CH_x are adsorbed onto the SWCNT(10,10) surface, three peaks appear at around 11, 14, and 17 Å. Before 50 ps, all the three peaks increase, the height of the second (14 Å) and the third peak (17 Å) decreases after 50 ps, and the third peak disappears after 200 ps, which may correspond to the adsorption process. From 200 to 2000 ps, the height of the first peak changes a little. This also shows us the two-stepped isothermal crystallization process.

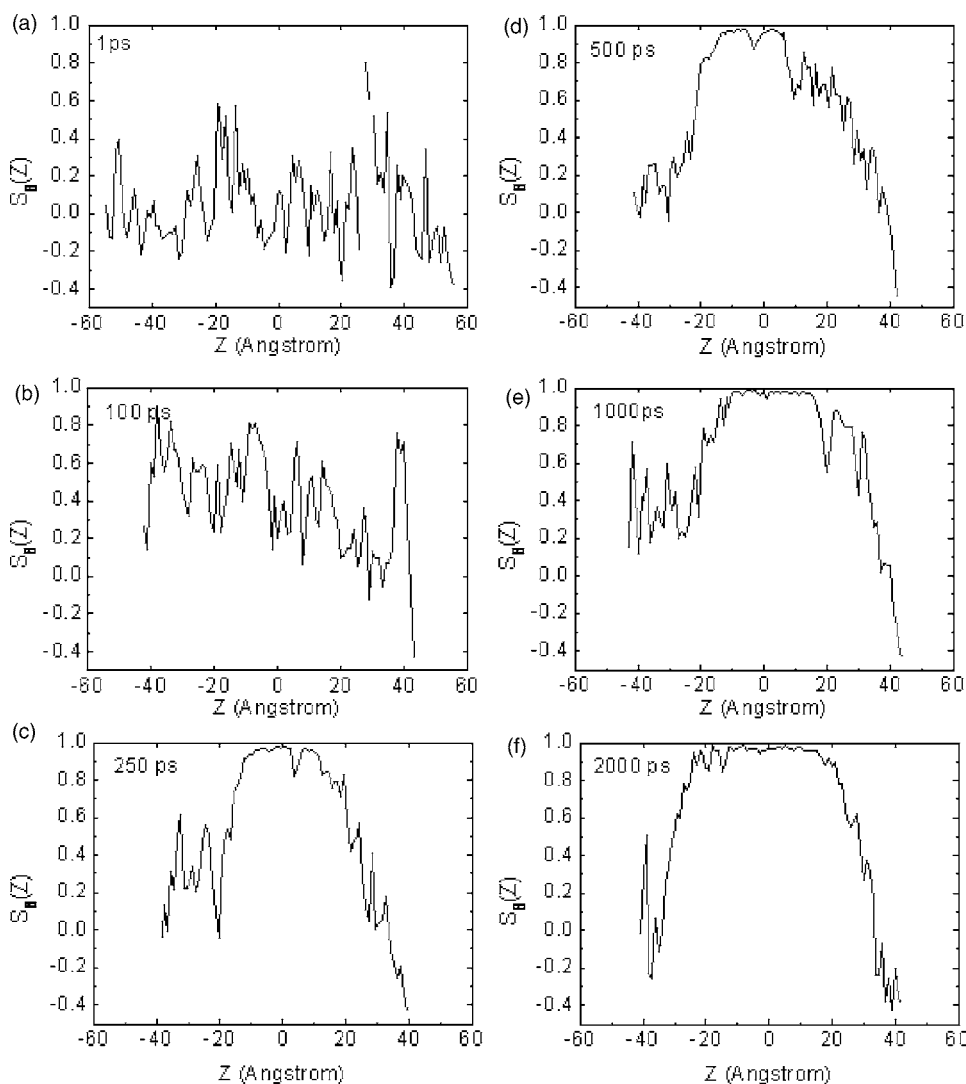


FIG. 4. Local bond-orientational order parameter $S_B(z)$ vs z at (a) $t=1$ ps, (b) $t=100$ ps, (c) $t=250$ ps, (d) $t=500$ ps, (e) $t=1000$ ps, and (f) $t=2000$ ps of PE500 on SWCNT(10,10).

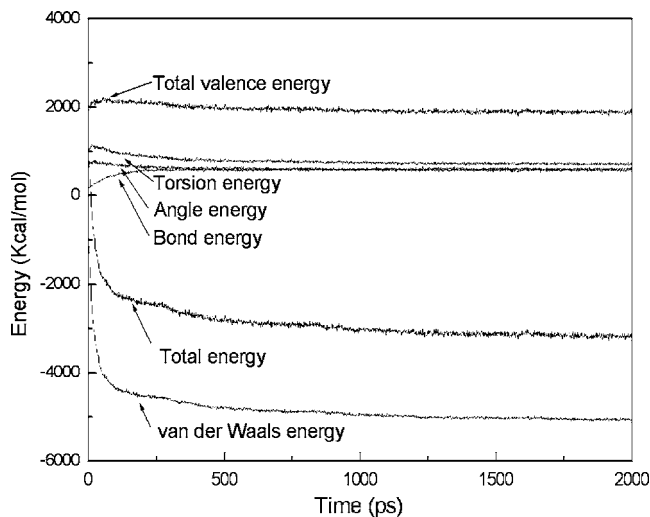


FIG. 5. Time evolution of total valence, torsion, angle, bond, van der Waals, and total potential energy of PE1000-10-10 system.

B. Bond-orientational order

To investigate the bond-orientational order of polymer chain of PE500-10-10 system, we firstly calculate the global bond-orientational order parameter A ,²⁰ which is defined by

$$A = \frac{1}{n-2} \sum_{i=3}^n \left\langle \frac{3 \cos^2 \psi_i - 1}{2} \right\rangle, \quad (2)$$

where ψ_i is the angle between the subbond vector \mathbf{b}_i and the z axis and $\mathbf{b}_i = (\mathbf{d}_i + \mathbf{d}_{i-1})/2$ is the vector formed by connecting centers of two adjacent bonds i and $i-1$, with \mathbf{d}_i the bond vector. The parameter A would assume a value of 1.0, 0.0, or -0.5 , respectively, for a polymer chain whose subbonds are perfectly parallel, random, or perpendicular to the z axis.

The time evolution of global bond-orientational order parameter A of PE500 on SWCNT(10,10) is plotted in Fig. 3. As can be seen in Fig. 3, A quickly increases from 0.0 to 0.55 before 150 ps, and then slowly increases to approximately 0.69 from 150 to 2000 ps. This phenomenon indicates that the single polymer chain transits from a random-coil to a bond-orientationally ordered structure, which also corresponds to a two-stepped mechanism in the relaxation of PE500 on the SWCNT surface.

In order to investigate the local bond-orientational order, we further calculate the local bond-orientational order parameter $S_B(z)$,²⁰ which is defined by

$$S_B(z) = \left\langle \left\langle \frac{3 \cos^2(\psi(z)) - 1}{2} \right\rangle_{\text{bond}} \right\rangle, \quad (3)$$

where $\psi(z)$ is the angle between the subbond vector \mathbf{b} in a slab $[z, z+dz]$ and the z axis, and $\langle \cdots \rangle_{\text{bond}}$ denotes the average over the subbonds in a slab between z and $z+dz$. The parameter $S_B(z)$ would assume a value of 1.0, 0.0, or -0.5 , respectively, for subbonds in a slab $[z, z+dz]$ perfectly parallel, random, or perpendicular to the z axis. We set $dz = 1.0 \text{ \AA}$ in our calculations of $S_B(z)$. Similar to Fujiwara and Sato,²⁰ we define an ordered domain as the region ($z_{\min}^s < z < z_{\max}^s$) where $S_B(z)$ is larger than 0.9. The average stem length is defined as $z_{\max}^s - z_{\min}^s$.

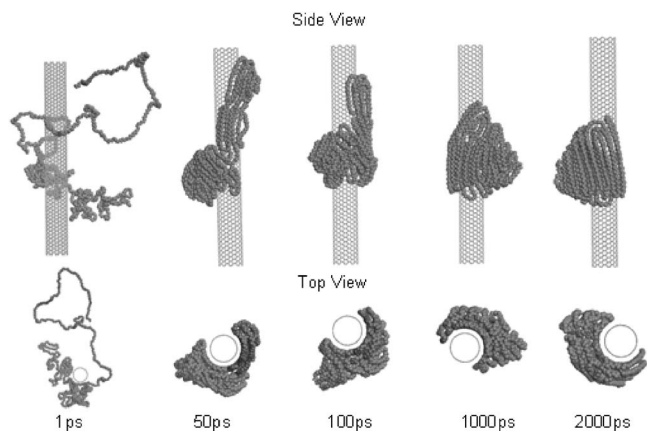


FIG. 6. Relaxation process of PE500 chain on SWCNT(10,10) surface at 300 K with relatively strong intramolecular (polymer-polymer) interactions.

Figure 4 shows the local bond-orientational order parameters $S_B(z)$ at $t=1, 100, 250, 500, 1000,$ and 2000 ps of PE500 on SWCNT(10,10). When $t=1$ ps [Fig. 4(a)], $S_B(z)$ is almost zero independent of z , which indicates that the PE chain is a random-coil structure. In the case of $t=100$ ps [Fig. 4(b)], $S_B(z)$ reaches 0.8 some times, which indicates a local orientationally ordered structure. When $t=250$ ps [Fig. 4(c)], $S_B(z)$ reaches 0.9. This means that a relatively orientationally ordered structure appears, and the average stem length of this structure is approximately 30 \AA . With the time further increasing [Figs. 4(d)–4(f)], the average stem length increases from approximately 30 to 50 \AA , indicating that the PE chain forms an ordered structure, as shown in Fig. 1.

By combining the above discussion, we can summarize the crystallization process as two stages. First, PE chain is adsorbed onto the SWCNT surface. The global bond-orientational order parameter increases quickly as time increases, but only local ordered structure appears in this stage. This stage ranges from 1 to 200 ps in our simulation of PE500-10-10 system. Second, the adsorbed chain orientates to an ordered lamellae. In this stage, the change of global bond-orientational order parameter is small, but the average stem length increases obviously.

C. Effect of energy on crystallization

Figure 5 shows the time evolution of total valence, torsion, angle, bond, van der Waals, and total potential energy of PE1000-10-10 system. We can see that, as the relaxation proceeds, the torsion, angle, and bond energies are repulsive (positive), while the van der Waals energy is attractive (negative). It is obvious that, during the relaxation process of PE1000-10-10, the total potential energy decreases due to the significant decrease of van der Waals energy. So like PE or PE-like polymers,^{23,25} the main driving force for PE adsorption and orientation on SWCNT is also the attractive van der Waals interactions. From Fig. 5, it can be seen that after 800 ps, total valence, torsion, angle, and bond energies fluctuate around a value, and the van der Waals and total potential energy still have a decreasing slope, which also show that van der Waals interactions are the main driving force for PE crystallization on SWCNT surface. The decreasing slope

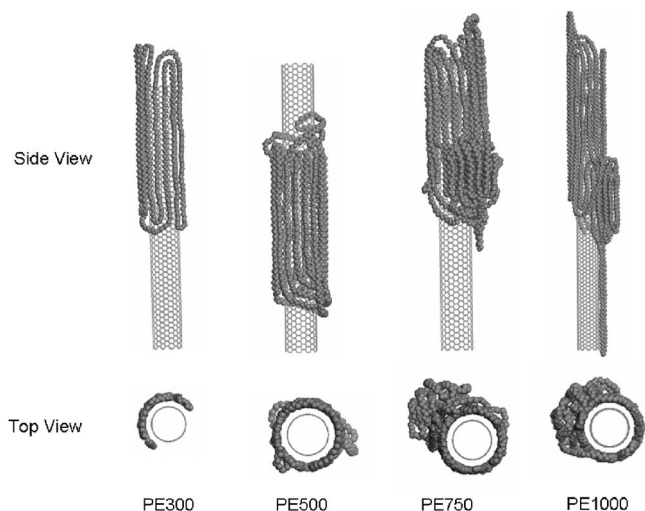


FIG. 7. Snapshots of the final conformation of PE with different chain lengths on SWCNT(10,10).

is very small, which means that the simulation time of 2000 ps is long enough for our systems to reach equilibrium.

The van der Waals energy between nonbonded atoms separated by more than two bonds is calculated by the 12-6 Lennard-Jones potential,

$$E_{LJ} = \sum_{i=1}^n \sum_{\substack{j=1 \\ (j-i \geq 3)}}^n 4\epsilon \left[\left(\frac{\sigma}{r_{ij}} \right)^{12} - \left(\frac{\sigma}{r_{ij}} \right)^6 \right], \quad (4)$$

where r_{ij} is the distance between atoms i and j . Well depth $\epsilon=0.1984$ kcal/mol, and repulsive wall $\sigma=0.36239$ nm in our simulations. In order to investigate the effect of van der Waals energy on crystallization, we change the well depth ϵ to 0.3968 kcal/mol, which equals to relatively increasing the intramolecular (polymer-polymer) van der Waals interac-

tions, and other simulation details are the same as before. A different crystallization process of PE500 on SWCNT(10,10) is shown in Fig. 6. PE500 chain is also adsorbed onto the SWCNT surface and forms an ordered structure, but the ordered structure is different from the result under a normal force field. The segments contacting the SWCNT surface is less than the normal result. The average stem length is also much shorter than the normal result. This shows us a different situation that a bad solvent leads to stronger chain collapse and thus shorter average stem length.

D. Ordered structure of different chain lengths

The coverage of PE on the SWCNT changes corresponds to the PE chain length. Figure 7 shows the snapshots of the final conformations of PE with different chain lengths on SWCNT(10,10). As can be seen in Fig. 7, the four PE chain lengths all form ordered structures whose stems align parallel to the SWCNT axis. The PE300 chain and PE500 chain form ordered monolayer structure, while the longer PE750 chain and PE1000 chain form ordered poly-layer-like structure on SWCNT surface. One fact in our simulation must be pointed out that there are two kinds of ordered structures for the PE300 (the stems parallel or incline to the SWCNT axis). The potential energy of the two kinds of structure is -1100.72 kcal/mol (paralleling to the SWCNT axis) and -1024.30 kcal/mol (inclining to the SWCNT axis). Thus, we choose the structure with lower potential energy, whose stems parallel to the SWCNT axis, as the last structure.

We also show the local bond-orientational order parameter $S_B(z)$ of PE300, PE500, PE750, and PE1000 on SWCNT(10,10) at 2000 ps in Fig. 8. This figure shows the following features. (a) The bond-orientational order parameter $S_B(z)$ in the flat regions of the four kinds PE chain all

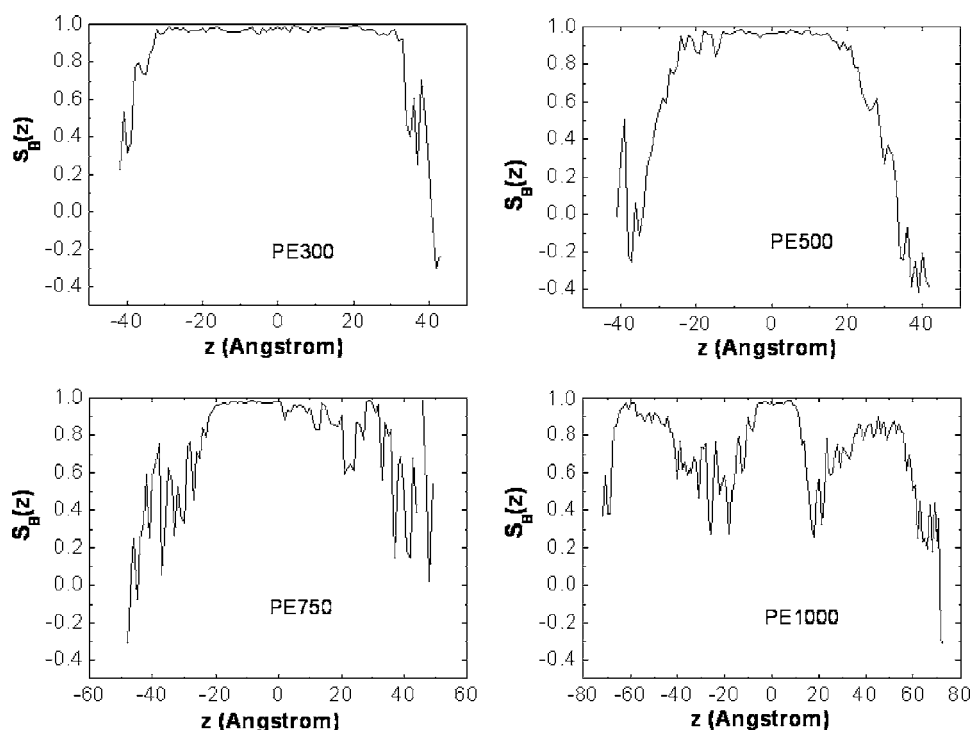


FIG. 8. Local bond-orientational order parameter $S_B(z)$ of PE300, PE500, PE750, and PE1000 on SWCNT(10,10) at 2000 ps.

reaches 0.9, which shows that the subbands in these regions are almost parallel to the SWCNT axis. (b) There is a big flat region in PE300, PE500, or PE750 which shows a global ordered structure. In addition, there is more than one flat region in PE1000, which gives a structure with some local ordered structure. This may be caused by the effect of his periodic image, which is shown in Fig. 7. (c) As the chain length increases, more microstructures appear in the last ordered structure.

IV. CONCLUSIONS

In this article, we studied the isothermal crystallization process of single PE chains with different chain lengths on SWCNT(10,10). The results show that there are two stages in the isothermal process. First, the PE chain is adsorbed onto the SWCNT surface. The global bond-orientational order parameter increases quickly as time increases, but only the local ordered structure appears in this stage. Second, the adsorbed chain orientates to an ordered lamellae. The average stem length increases obviously in this stage. The attractive van der Waals interactions control the PE adsorption and orientation on SWCNT. The stems of the ordered structure align parallel to the SWCNT axis, and as the chain length increases, more microstructures appear in the last ordered structure.

ACKNOWLEDGMENTS

We are grateful to 973 Program (2006CB932900), NNSFC (Nos. 90306009 and 20421202), and Postdoctoral Science Foundation of China for financial support.

¹S. Iijima, *Nature* (London) **354**, 56 (1991).

²A. Thess, R. Lee, P. Nikolaev, H. J. Dai, P. Petit, J. Robert, C. H. Xu, Y. H. Lee, S. G. Kim, A. G. Rinzler, D. T. Colbert, G. E. Scuseria, D. Tomanek, J. E. Fischer, and R. E. Smalley, *Science* **273**, 483 (1996).

³S. J. Tans, M. H. Devoret, H. J. Dai, A. Thess, R. E. Smalley, L. J. Geerligs, and C. Dekker, *Nature* (London) **386**, 474 (1997).

⁴M.-F. Yu, M. J. Dyer, and R. S. Ruoff, *J. Appl. Phys.* **89**, 4554 (2001).

⁵M. Ouyang, J.-L. Huang, and C. M. Lieber, *Acc. Chem. Res.* **35**, 1018 (2002).

⁶A. Javey, J. Guo, Q. Wang, M. Lundstrom, and H. Dai, *Nature* (London) **424**, 654 (2003).

⁷R. J. Chen, Y. G. Zhan, D. W. Wang, and H. J. Dai, *J. Am. Chem. Soc.* **123**, 3838 (2001).

⁸E. Katz and I. Willner, *ChemPhysChem* **5**, 1085 (2004).

⁹M. J. O'Connell, P. Boul, L. M. Ericson, C. Huffman, Y. H. Wang, E. Haroz, C. Kuper, J. Tour, K. D. Ausman, and R. E. Smalley, *Chem. Phys. Lett.* **342**, 265 (2001).

¹⁰L. Y. Li, C. Y. Li, and C. Y. Ni, *J. Am. Chem. Soc.* **128**, 1692 (2006).

¹¹L. Y. Li, Y. Yang, G. L. Yang, X. M. Chen, B. S. Hsiao, B. Chu, J. E. Spanier, and C. Y. Li, *Nano Lett.* **6**, 1007 (2006).

¹²L. Mandelkern, *Crystallization of Polymers* (McGraw-Hill, New York, 1964).

¹³R. G. Alamo and L. Mandelkern, *Macromolecules* **22**, 1273 (1989).

¹⁴K. Armitstead and G. Goldbeck-Wood, *Adv. Polym. Sci.* **100**, 219 (1992).

¹⁵M. H. Kim and P. J. Philips, *J. Appl. Polym. Sci.* **70**, 1893 (1998).

¹⁶M. Muthukumar, *Eur. Phys. J. E* **3**, 199 (2000).

¹⁷G. Strobl, *Eur. Phys. J. E* **3**, 165 (2000).

¹⁸G. Strobl, *Prog. Polym. Sci.* **31**, 398 (2006).

¹⁹T. A. Kavassalis and P. R. Sundararajan, *Macromolecules* **26**, 4144 (1993).

²⁰S. Fujiwara and T. Sato, *J. Chem. Phys.* **107**, 613 (1997).

²¹X. B. Zhang, Z. S. Li, Z. Y. Lu, and C. C. Sun, *J. Chem. Phys.* **115**, 10001 (2001).

²²S. Fujiwara and T. Sato, *J. Chem. Phys.* **114**, 6455 (2001).

²³X. B. Zhang, Z. S. Li, Z. Y. Lu, and C. C. Sun, *J. Chem. Phys.* **115**, 3916 (2001).

²⁴X. B. Zhang, Z. S. Li, Z. Y. Lu, and C. C. Sun, *Macromolecules* **35**, 106 (2002).

²⁵X. B. Zhang, Z. S. Li, H. Yang, and C. C. Sun, *Macromolecules* **37**, 7393 (2004).

²⁶H. X. Guo, X. Z. Yang, and T. Li, *Phys. Rev. E* **61**, 4185 (2000).

²⁷H. Meyer and F. Müller-Plathe, *J. Chem. Phys.* **115**, 7807 (2001).

²⁸H. Meyer and F. Müller-Plathe, *Macromolecules* **35**, 1241 (2002).

²⁹M. J. Ko, N. Waheed, M. S. Lavine, and G. C. Rutledge, *J. Chem. Phys.* **121**, 2823 (2004).

³⁰C. Liu and M. Muthukumar, *J. Chem. Phys.* **109**, 2536 (1998).

³¹I. Dukovski and M. Muthukumar, *J. Chem. Phys.* **118**, 6648 (2003).

³²M. Muthukumar, *Adv. Polym. Sci.* **191**, 241 (2005), and references therein.

³³T. Yamamoto, *J. Chem. Phys.* **125**, 064902 (2006).

³⁴T. Yamamoto, *Adv. Polym. Sci.* **191**, 37 (2005), and references therein.

³⁵L. Toma, S. Toma, and J. A. Subirana, *Macromolecules* **31**, 2328 (1998).

³⁶J. P. K. Doye and D. Frenkel, *Phys. Rev. Lett.* **81**, 2160 (1998).

³⁷G. Xu, H. Lin, and W. L. Mattice, *J. Chem. Phys.* **119**, 6736 (2003).

³⁸M. J. Yang, V. Koutsos, and M. Zaiser, *J. Phys. Chem. B* **109**, 10009 (2005).

³⁹S. L. Mayo, B. D. Olafson, and W. A. Goddard III, *J. Phys. Chem.* **94**, 8897 (1990).

⁴⁰L. Verlet, *Phys. Rev.* **159**, 98 (1967).

⁴¹S. Nosé, *Mol. Phys.* **52**, 255 (1984).

⁴²S. Nosé, *J. Chem. Phys.* **81**, 511 (1984).

⁴³Q. Liao and X. Xin, *J. Chem. Phys.* **110**, 8835 (1999).

⁴⁴See EPAPS Document No. E-JCPSA6-127-006732 for our additional MD simulation results of the PE1500 on SWCNT(10,10) surface. This document can be reached through a direct link in the online article's HTML reference section or via the EPAPS homepage (<http://www.aip.org/pubservs/epaps.html>).